

A Robust Multi-pass Printing Method

Cesar L. Nino and T. Roger Keane III; E.I duPont de Nemours; Wilmington, Delaware, U.S.A.

Abstract

In this paper, a robust multi-pass printing method is introduced. This is a technique where a new design variable is included: a weight factor $A(n)$ that affects the density of dots being printed by every nozzle in the print-head. In the paper, the dot density of a vertical multi-pass system is described in an analytical expression. Then, it is theoretically shown how the minimization of the roughness measure of above expression with respect to $A(n)$ leads to a closed expression for the optimal dot density at every pass, or, in other words, to the optimal multi-pass system.

Introduction

A key aspect on the design of an inkjet printer is the multi-pass system, sometimes called interlace system, which allows the printer to achieve higher resolutions in the vertical and horizontal directions with a lower resolution print head. The basic idea behind multi-pass printing is to divide the number N of available nozzles of the print head in a number of sectors K that acts as the multiplier of the printing resolution. Vertical interlacing, however, only performs well as long as the media transport mechanism works properly. Many times the advancing steps of the media have small, microscopic offsets mostly due to slippage between transport and substrate. This source of error introduces an artifact commonly known as banding, from the fact that it shows as a fairly regular pattern with periodicity exactly equal to the size of the printing bands. The manufacturers of desktop inkjet printers usually calibrate their hardware to mitigate the effect of banding for their recommended media. The problem with large format printers is that the media substrates may vary drastically from one print to the next, for example from paper-thin vinyl to 1/8-inch PVC board, thus making it virtually impossible to compensate for the error only mechanically. Therefore, and in addition to the necessary mechanical adjustments to the printer, the system requires the multi-pass printing system to be robust enough to compensate for inaccuracies as much as possible. In this paper, a robust multi-pass printing method is introduced. This is a technique where a new design variable is included: a weight factor $A(n)$ that affects the density of dots being printed by every nozzle in the print head. This work starts by describing the dot density of a vertical multi-pass system in an analytical expression. Then, it is shown how the minimization of the roughness measure of above expression with respect to $A(n)$ leads to a closed expression for the optimal dot density at every pass, or, in other words, to the optimal multi-pass system. Visual results are included to show the dramatic difference in image quality between conventional multi-pass and robust multi-pass in a real large-format printing system.

Multipass Printing

An important part of any inkjet printer is its multipass system, which allows the printer to achieve high resolutions in the vertical direction with a lower resolution print head. The basic

idea behind multipass printing is to divide the number N of available nozzles in the print head in a number of sectors K_y that will act as the multiplier of the printing resolution. More precisely, let us denote the final printing resolution as R_f and the original print head resolution as R_o . The number of sectors in which the nozzles need to be divided is $K_y = \frac{R_f}{R_o}$. A further condition is that K_y must be an integer, or, in other words, R_f can only be a multiple of the original resolution R_o . Once the print head is divided in sectors (of the same size), the multipass printing algorithm can be described as follows.

1. Set $m = 0$. m keeps the count of the number of passes over the entire image.
2. The media advances a distance $S = m \times \frac{\Delta y \times N}{K_y} - O_y$, where Δy is the distance between two adjacent nozzles, i.e. the reciprocal of the actual print head resolution, and N is a multiple of K_y . The term $O_y = \frac{\text{mod}(m, K_y) \times \Delta y}{K_y}$ is the offset term that actually places the nozzles slightly delayed every time, thus achieving a higher printing resolution.
3. Print using all the nozzles.
4. Set $m = m + 1$. Go to step 2.

The image is printed in sections or *bands* that get completed whenever the print head has passed K_y times over that region of the media. Since the first and the last $K_y - 1$ bands do not complete the minimum number of passes they cannot be used to print image data. Instead, a zero padding is used in those regions as it is shown in Fig. 1.

It is not hard to realize that the same multipass principle can be used to increase the resolution on the horizontal direction as well, by simply addressing every line a number of times $K_x > 1$. In such case, K_x acts as the horizontal resolution multiplier, and therefore the print head needs to be divided in $K_x \times K_y$ equally-sized sectors. The algorithm described above may be modified to account for K_x in the following manner:

1. Set $m = 0$.
2. The media advances a distance $S = m \times \frac{\Delta y \times N}{K_y \times K_x} - O_y$, where Δy is still the distance between two adjacent nozzles and N is a multiple of $K_y * K_x$. The term O_y remains as previously defined.
3. Print using all the nozzles starting at an offset $O_x = \frac{\text{mod}(m, K_x) \times \Delta x}{K_x}$.
4. Set $m = m + 1$. Go to step 2.

Before analyzing the problems that multipass printing faces, it is necessary to express the process in a mathematical way. In

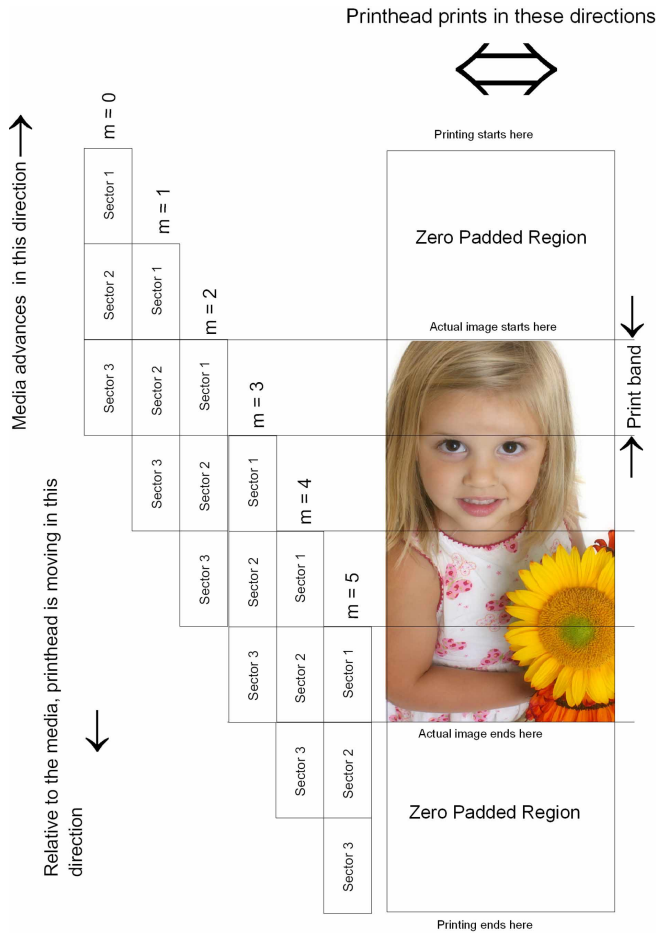


Figure 1. In this example the span of a print head has been divided in three sectors ($K_y = 3$), and the entire image has been covered in 6 passes. The image is divided in 8 bands, from which the first and the last 2, corresponding to $(K_y - 1)$ cannot be used for printing (zero padded regions).

order to simplify the analysis, this description could involve only variables along one dimension. For simplicity, let us define the profile of the print head as the composition of the cross-sections of the dots, i.e. the dot profiles¹ that are printed by the nozzles at the positions that the multipass algorithm indicates:

$$I(y) = \sum_{m=0}^M \sum_{n=0}^{N-1} P(y - n \cdot \Delta y - m \cdot S + O_m), \quad (1)$$

where $S = \frac{\Delta y \cdot N}{K_y \cdot K_x}$, and $O_m = \frac{\text{mod}(m, K_y) \cdot \Delta y}{K_y}$. Here M represents the total number of passes, and the function $P(y)$ represents the one dimensional dot profile. This definition needs to be completed further by adding the fact that the human visual system works as a low-pass filter, hence

$$I(y) = \sum_{m=0}^M \sum_{n=0}^{N-1} P_h(y - n \cdot \Delta y - m \cdot S + O_m)$$

with $P_h(y) = P(y) * h(y)$, where $h(y)$ is the human visual system response. Fig. 2 shows a simple dot profile that we can use to

¹The simplest dot profile could be a square pulse

describe multipass printing.

Sometimes the process of multipass printing is also called

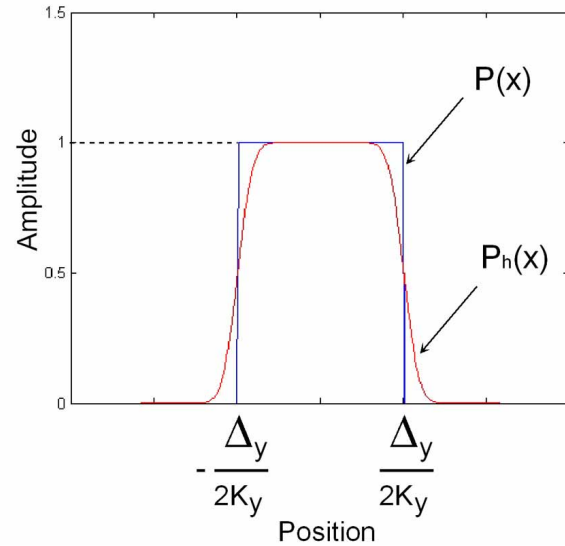


Figure 2. The square pulse $P(x)$ describes a dot profile, which is the view of a cross section of a dot along the vertical (or horizontal) printing axis. The function $P_h(x)$ is the same dot profile after being convolved with the human visual response.

interlace, and the parameters K_y and K_x replaced by their indexes. Likewise, some people specify a printing mode by referring to the number of passes needed to fill a band and the type of interlace that is being used. For example, a way to describe a printing mode could be: 12-pass mode, with X-interlace = 3 and Y-interlace = 4. This way of describing multipass printing is rather common and will be used in further sections.

Banding

Multipass printing works extremely well as long as the print head, the media transport mechanism, and the nozzles work properly. Many times, however, the nozzles clog, the print head is misaligned, and the media steps have small, microscopic offsets. All of these sources of error introduce an artifact called *banding* from the fact that it shows as a fairly regular line pattern with periodicity exactly equal to the length of the printing bands. Assuming that the print head is calibrated and properly aligned, the effects of faulty nozzles and media transport can be lessened by using X-interlace. In the case of faulty nozzles, the logic behind the use of X-interlace is very simple: by using more than one nozzle to address the same line, the probability of having empty lines in the printed image will be smaller. It is also possible to design the interlace to minimize the banding coming from offset errors. Figures 3 and 4 show the effects of multipass printing in an ideal printer and in a printer with some error offset in the media transport system. The same figures show the relationship between the mathematical model defined above and image quality in both scenarios. In the latter case, when errors are introduced, equation

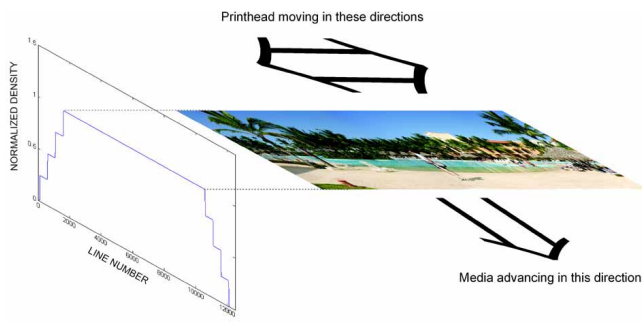


Figure 3. In this figure we illustrate the 1-D model. In a perfect printer the multipass system produces a smooth and flat dot-density response.

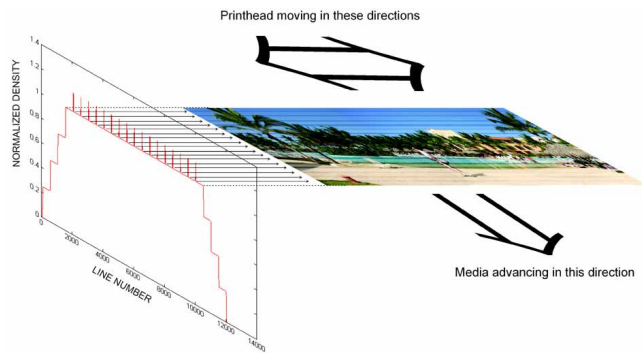


Figure 4. A printer exhibits banding when some error affects the media transport system. This can be 1-D modeled as a periodic increase in density on certain regions of the image.

(1) becomes

$$I(y) = \sum_{m=0}^M \sum_{n=0}^{N-1} P_h(y - n \cdot \Delta y - m \cdot S + O_m + \eta),$$

where the term η denotes the microscopic error at every pass. All other terms in the expression remain as defined above. Essentially, media transport systems are rolling devices (pinch-rollers and a drive roller or a belt) that use the friction against the media to accurately transport it. A vacuum system helps to hold the media in-place during the print, and gives more stability when transporting the media from pass to pass. The greater contributor to offsets then, is the inertia of the substrate which causes slippage between media and rollers. In order to prevent this, printers usually are calibrated by the manufacturer to compensate the excess play for a recommended set of substrates. In high-accuracy systems the substrates are designed such that some physical properties, like media curling, are optimized for the internal mechanism. The problem with large format printers is that the media substrate may change drastically in dimension and weight from one print to the next. Therefore, and in addition to the necessary adjustments in the vacuum pressure that holds the media attached to the moving belt, the system requires the multipass printing to be robust enough to compensate for inaccuracies as much as possible. Although the error η has a strong deterministic origin, it is still considered a non-zero mean, independent gaussian random variable, where both parameters,

mean and variance are much smaller than the nozzle-to-nozzle spacing ($\mu_\eta \ll \Delta y, \sigma_\eta \ll \Delta y$). This latter condition makes η appear as a nearly constant value for the duration of the print, i.e. causing the banding to be quasi-periodic.

Robust Multipass

Before starting the analysis, it will be assumed that the Y -interlace is equal to one ($K_y = 1$), which is an assumption that by no means affects the generality of the analysis, but it rather simplifies the use of some terms. From the algorithms described in the previous section, as well as from the expression above for $I(y)$, it is apparent that the density of dots at every pass is a constant across the nozzles in the print head. More precisely, the density at every pass must be $1/K_x$ in order to complete every band in the image. For instance, a multipass system with X -interlace = 2 prints 50% of the dots in one pass and the other 50% in the next and so forth until it finishes printing the image. In reality, the density of dots across the print head could take any form as long as 100% of the dots in the band have been printed after K_x passes. In order to take advantage of this, a new variable is introduced, a weight factor A_n that affects the density of dots being printed by every nozzle. Recalling a former expression, the mathematical description of multipass printing becomes

$$I(y) = \sum_{m=0}^M \sum_{n=0}^{N-1} A_n \cdot P_h(y - n \cdot \Delta y - m \cdot S + O_m + \eta), \quad (2)$$

under the constraint that

$$\sum_{n=0}^{\frac{N}{K_x}-1} \sum_{k=0}^{K_x-1} A_{n+\frac{k \cdot N}{K_x}} = 1.$$

Notice that A_n describes a discrete set of N numbers, one per nozzle, in the range $[0..1]$. Minimization of the roughness measure of equation (2) with respect to A_n leads to the optimal weights for every pass, or, in other words, to the optimal multipass. Roughness of an arbitrary function $f(y)$, as classically defined in the literature is

$$R = \int_a^b \left(\frac{\partial^j f(y)}{\partial y^j} \right)^2 dy,$$

where the range $[a..b]$ is the domain of the function. In our case, that domain is the region between the actual start and the end of the image, i.e. excluding the zero-padding zones. The order j of the partial derivative controls the degree of smoothness, that is greater smoothness is achieved with higher order derivatives. The problem of finding the optimal A_n is stated as

$$A_{n_{optim}} = \min_{A_n} E \left\{ \int_a^b \left(\frac{\partial^j I(y, A_n, \eta)}{\partial y^j} \right)^2 dy \right\},$$

where $E \{ \cdot \}$ is the statistical expectation operator. Under the assumptions that $N - 1 \gg 1, \Delta y \rightarrow 0$ and $(N - 1) \times \Delta y = L$, where L is the physical length of the print head measured from the first to the last nozzle, and also rearranging some terms, equation(2) transforms into

$$I(y) = P_h(y + \eta) * \sum_{m=0}^M A(y - m \frac{L}{K_x}), \quad (3)$$

where $A(y)$ has become a continuous function. Now, evaluation of roughness in this expression is somewhat straightforward if we include the integrals from the definition of convolution. Rearranging the terms, and integrating over a sufficiently large distance, that is, making $a \rightarrow -\infty$, $b \rightarrow \infty$

$$R = E \left\{ \int_{-\infty}^{\infty} P_h(t + \eta) \int_{-\infty}^{\infty} P_h(\tau + \eta) \int_{-\infty}^{\infty} \psi_j(y - t, y - \tau) dy d\tau dt \right\},$$

where

$$\psi_j(y - t, y - \tau) = \sum_{v=0}^M \frac{\partial^j A(y - v \frac{L}{K_x} - t)}{\partial y^j} \sum_{u=0}^M \frac{\partial^j A(y - u \frac{L}{K_x} - \tau)}{\partial y^j}.$$

Using the substitution $\hat{y} = y - t$

$$R = E \left\{ \int_{-\infty}^{\infty} P_h(t + \eta) \int_{-\infty}^{\infty} P_h(\tau + \eta) \int_{-\infty}^{\infty} \psi_j(\hat{y}, \hat{y} + t - \tau) d\hat{y} d\tau dt \right\}.$$

Now, substituting $\lambda = \tau - t$, and rearranging the terms

$$R = \int_{-\infty}^{\infty} \hat{\Phi}_{P_h}(\lambda) \int_{-\infty}^{\infty} \psi_j(\hat{y}, \hat{y} - \lambda) d\hat{y} d\lambda, \quad (4)$$

with

$$\hat{\Phi}_{P_h}(\lambda) = E \left\{ \int_{-\infty}^{\infty} P_h(t + \eta) P_h(\lambda + t + \eta) dt \right\}.$$

In a variational approach, equation (4) is the definition of a weighted smoothing spline, where the weight function is given by the autocorrelation of the dot profile $P_h(\lambda)$, i.e. $\hat{\Phi}_{P_h}(\lambda)$. The solution of this problem depends greatly on the shape of P_h ; implementation could easily turn cumbersome, and therefore not practical. However, the more serious drawback, in terms of robustness, is still the direct dependence on η . Two practical conditions facilitate the task of finding a more robust yet optimal function $A(y)$. The first condition is that the dot profile P_h is a function with a finite width $\Delta = \Delta_y / K_x$, and that the width itself is much smaller than the size of the print head ($\Delta \ll L$) which is the compact support of the function $A(y)$. This is easy to see in practice: a printed dot usually has a diameter no bigger than 100 microns while the length L of a print head typically measures several centimeters, this means that in many cases the ratio L/Δ reaches two orders of magnitude. The second condition is that the mean and the variance of the offset term η are in the microscopic range, and they are much smaller than the interspace between scanlines, i.e. $\mu_\eta \ll \Delta$, $\sigma_\eta \ll \Delta$. Under these conditions, the function $\hat{\Phi}_{P_h}(\lambda)$ approximates to a *Dirac's delta*². Using the appropriate mathematical properties, equation (4) then reduces to

$$R \approx \int_{-\infty}^{\infty} \sum_{v=0}^M \frac{\partial^j A(y - v \frac{L}{K_x})}{\partial y^j} \sum_{u=0}^M \frac{\partial^j A(y - u \frac{L}{K_x})}{\partial y^j} dy. \quad (5)$$

The function $A(y)$ that minimizes equation (5) can be found in the literature[1, 2, 3], and it is the polynomial spline of order j , also known as the *polynomial B-spline* of order j . Polynomial B-splines are symmetrical functions that could be defined in many ways, but a very succinct and useful definition is found in

²see Appendix section

[4, 5]. Schoenberg's definition of a real, symmetrical polynomial B-spline of order j is

$$A_j(y) = \sum_{i=0}^{j+1} \frac{(-1)^i}{j!} \binom{j+1}{i} \left(y + \frac{j+1}{2} - i\right)^j \cdot U\left(y + \frac{j+1}{2} - i\right), \quad (6)$$

where

$$U(y) = \begin{cases} 0 & : y < 0 \\ 1 & : y \geq 0. \end{cases}$$

In order to comply with the aforementioned constraint that

$$\sum_{n=0}^{\frac{N}{K_x} - 1} \sum_{k=0}^{K_x - 1} A_{n+k, \frac{N}{K_x}} = 1,$$

the order of the B-spline must be $j = K_x - 1$. This is in accord with the fact that an X -interlace of higher order (i.e. a higher B-Spline order) produces a smoother appearance.

In practice, the actual density of dots used in the multipass must be a sampled version of $A_j(y)$, where samples occur at every nozzle position. Of course, the domain of the B-spline also has to equal the length of the print head, which means that the optimal set of weights for the multipass uses the definition of a B-spline that fits perfectly on L , as shown in Fig. 6. Sampling the B-spline from equation (6), after scaling and shifting, yields the optimal multipass weights

$$A_n = \sum_{i=0}^{K_x} \frac{(-1)^i}{(K_x - 1)!} \binom{K_x}{i} \left(n + \frac{K_x - N}{2} - i\right)^{K_x} \cdot U\left(\frac{n + \frac{K_x - N}{2} - i}{\frac{N}{K_x}}\right), \quad (7)$$

that is, the optimal density of dots to be printed by the n^{th} nozzle

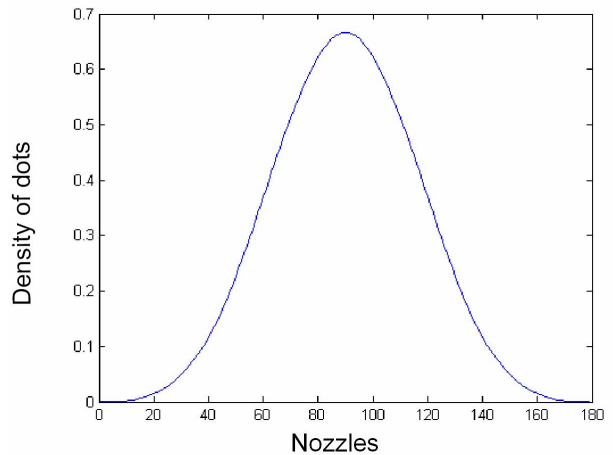


Figure 6. An illustration of the shape of the optimal weights in a 180-nozzle multipass printing system, with $K_x = 4$

($n \in [0..N - 1]$) in a mode with K_x passes. Notably, a zero-order

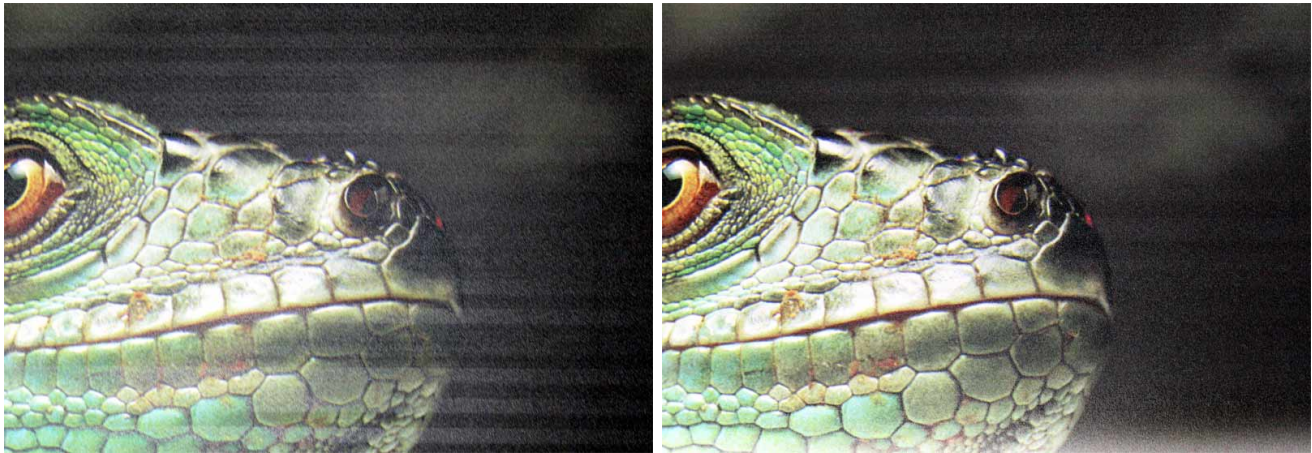


Figure 5. A visual example of robust multipass, in which the image "Iguana" has been printed using an X-interlace mode = 2, first using the conventional multipass algorithm (left) and then using robust multipass (right).

spline is not suitable for multipass, since it implies no overlapping of passes, i.e. $K_x > 1$. Also, it needs to be remarked that taking into account the number of passes K_y for the Y-interlace does not modify the expression above. Fig. 6 illustrates the distribution of weights in an optimal multipass system. Likewise, Fig. 7 shows the effect of optimal versus conventional multipass printing.

Results

As a demonstration of the method, Figure 5 shows two prints from a large format printer, with and without robust multipass. It is apparent that the print that does not use robust multipass suffers from a type of banding that appears as streaks, of regions with different glossiness. The print with robust multipass shows a great reduction of this problem.

Also in this final section, two findings on optimal weighted multipass need to be commented. A first finding, through direct observation, is on the general shape of the weights. From the results above, it is notable that as the order of the B-spline increases, the use of the nozzles at each end of the print head approaches to zero, and this leads to inefficiency, particularly on the distribution of power when firing the nozzles at every pass. Whether this is a real drawback or not remains a matter of further investigation. A second finding on weighted multipass is that, albeit the smoothness of the results, it introduces a little deviation in the final density of the print, as it is shown in the detail of Fig. 7. This deviation is very small, nonetheless, it deserved a little more investigation, for the sake of color consistency. Through simulations it was determined that the deviation is a linear function (with negative slope) of the offset η and that it increases linearly with the order of the B-spline. The slope of the density change is in turn a non-linear function (exponential) that decreases with the size of the printband. Since the deviation is a function of the offset error η , the direct consequence might be the introduction of random variations in the final color of the print, i.e. color inconsistencies from print to print. Both findings lead to the same conclusion: weighted multipass is an

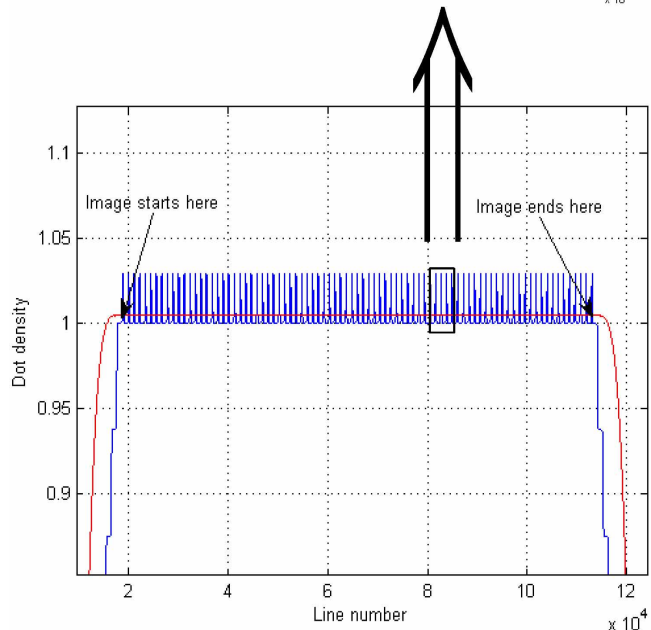
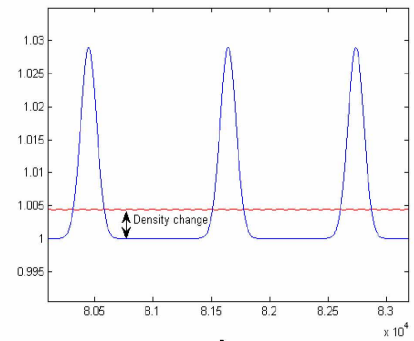


Figure 7. Robust multipass smooths the print dramatically

effective mechanism to reduce banding and improve dramatically the quality of printing, however, it is preferable to use lower order B-spline weights, especially when the goal is to keep

color consistency under certain tolerance. However, we need to mention that in our tests, good results in terms of color consistency and smoothness were always attained with interlaces of order $K_x \leq 6$.

References

- [1] J. C. Holladay, "A smoothest curve approximation," *Math. Tables Aids Comput.* **11**, pp. 233–243, 1957.
- [2] C. deBoor, "Best approximation properties of splines functions of odd degree," *J. Mech. Math.* **12**, pp. 747–749, 1963.
- [3] G. Micula, "A variational approach to spline functions theory," *Rend. Sem. Mat. Univ. Pol. Torino* **61**, pp. 209–227, 2003.
- [4] I. J. Schoenberg, "cardinal interpolation and spline functions," *Journal of Approximation Theory* **2**, pp. 167–206, 1969.
- [5] M. Unser, "B-spline signal processing: Part one - theory," *IEEE. Trans. On Signal Proc.* **41**, pp. 821–832, February 1993.

Appendix

Rigorously, the function $\Phi_{P_h}(\lambda)$ needs to be a nascent delta function, in the sense that

$$\lim_{\Delta \rightarrow 0} \int_{-\infty}^{\infty} \Phi_{P_h}(\lambda, \Delta) f(\lambda) d\lambda = f(0),$$

for all continuous $f(\cdot)$. Here, $2\Delta = \Delta_y/K_y$ is the compact support of Φ_{P_h} . Since the integral only take values in the neighborhood of zero, we can start by replacing $f(\cdot)$ by its Maclaurin series, that is

$$\begin{aligned} & \lim_{\Delta \rightarrow 0} \int_{-\Delta}^{\Delta} \Phi_{P_h}(\lambda, \Delta) \sum_{n=0}^{\infty} \frac{1}{n!} f^{(n)}(0) \lambda^n d\lambda \\ = & \lim_{\Delta \rightarrow 0} \sum_{n=0}^{\infty} \frac{1}{n!} f^{(n)}(0) \int_{-\Delta}^{\Delta} \Phi_{P_h}(\lambda, \Delta) \lambda^n d\lambda \end{aligned}$$

where the limits of the integral have already been replaced, and the term $f^{(n)}$ represents the n th derivative of $f(\cdot)$. By definition, the autocorrelation Φ_{P_h} is an even function, that is $\Phi_{P_h}(x) = \Phi_{P_h}(-x)$, therefore all *odd* terms (*n odd*) in the summation vanish, and the expression above reduces to

$$\lim_{\Delta \rightarrow 0} f(0) + \sum_{n=1}^{\infty} \frac{1}{(2n)!} f^{(2n)}(0) \int_{-\Delta}^{\Delta} \Phi_{P_h}(\lambda, \Delta) \lambda^{2n} d\lambda,$$

where, by convenience, we have assumed that

$$\int_{-\Delta}^{\Delta} \Phi_{P_h}(\lambda, \Delta) d\lambda = 1.$$

Recalling that $P_h(x) = P(x) * h(x)$, and assuming that the H.V.S model $h(x)$ is a smooth continuous function, for instance a gaussian function, then

$$\begin{aligned} \Phi_{P_h}^{(i)}(x) &= P_h(x) \otimes P_h^{(i)}(x) \\ &= P_h(x) \otimes (h^{(i)}(x) * P(x)), \end{aligned}$$

where \otimes and $*$ denote the correlation and convolution operators, respectively. From this result we can conclude that the derivatives of $\Phi_{P_h}(x)$ exist and therefore we can replace it by its Maclaurin expansion as well. The expression of the limit becomes

$$\begin{aligned} & \lim_{\Delta \rightarrow 0} f(0) + \sum_{n=1}^{\infty} \frac{1}{(2n)!} f^{(2n)}(0) \int_{-\Delta}^{\Delta} \sum_{k=0}^{\infty} \frac{1}{k!} \Phi_{P_h}^{(k)}(0) \lambda^{2n+k} d\lambda \\ = & \lim_{\Delta \rightarrow 0} f(0) + \sum_{n=1}^{\infty} \frac{f^{(2n)}(0)}{(2n)!} \sum_{k=0}^{\infty} \frac{\Phi_{P_h}^{(k)}(0) \Delta^{2n+k+1} (1 - (-1)^{2n+k+1})}{k!(2n+k+1)} \\ = & f(0), \end{aligned} \tag{8}$$

proving that Φ_{P_h} is a nascent delta. In the final step, we need to evaluate the expectation operator

$$\begin{aligned} \hat{\Phi}_{P_h}(\lambda) &= E \{ \Phi_{P_h}(\lambda + \eta) \} \\ &= \int_{-\infty}^{\infty} \Phi_{P_h}(\lambda + \eta) \frac{1}{\sqrt{2\pi}\sigma_\eta} e^{-\frac{(\eta-\mu_\eta)^2}{2\sigma_\eta^2}} d\eta. \end{aligned}$$

Since, in general, $\sigma_\eta \ll \Delta$, the gaussian curve behaves also as a nascent delta in this integral (i.e gaussians are well-known nascent delta functions); using the result in (8) and the practical fact that $\mu_\eta \ll \Delta$ as well, the expression above becomes

$$\begin{aligned} \hat{\Phi}_{P_h}(\lambda) &= \Phi_{P_h}(\lambda + \mu_\eta) \\ &= \delta(\lambda + \mu_\eta) \\ &\approx \delta(\lambda). \end{aligned}$$

Author Biography

Cesar L. Nino was born in Tunja, Colombia in South America. He received the degree of electronic engineer from the Xaverian Pontifical University at Bogota (1996) and the M.S. and Ph.D degrees in Electrical and Computer Engineering from the University of Delaware (2001,2003). Since then he works with the imaging technologies group at DuPont in Wilmington, DE. His work has been involved in the design and implementation of color processing algorithms, printer characterization models and halftoning methods.

T. Roger Keane III received his BS and MS degrees in Computer and Information Science from the University of Delaware (1981, 1985), and is a member of the IEEE. Since 1987, he has worked for Blair Computing Systems, Inc. providing software development services in a variety of markets, specializing in multi-platform applications for imaging, networking, analytical instrumentation and device control.